



Enhanced Energy Density of PANI/Co₃O₄/Graphene Ternary Nanocomposite in a Neutral Aqueous Electrolyte of Na₂SO₄ for Supercapacitor Applications

Shabhe Haider¹ · Imran Murtaza^{1,2} · Ahmed Shuja² · Rehan Abid¹ · Hasan Ali^{1,3} · Muhammad Adeel Asghar⁴ · Yaqoob Khan³

Received: 5 April 2022 / Accepted: 21 June 2022 / Published online: 9 July 2022
© The Minerals, Metals & Materials Society 2022

Abstract

We report a cost-effective, chemical polymerization route to synthesize PANI/Co₃O₄/graphene (PCG) ternary nanocomposite for supercapacitor applications to achieve enhanced energy density in a cost-effective, non-toxic, and non-corrosive neutral aqueous electrolyte of 1M Na₂SO₄. These properties are advantageous for a supercapacitor assembling procedure, being favorably facile and inexpensive. The electrochemical analysis was carried out to check analyte performance with cyclic voltammetry (CV), galvanostatic charge–discharge (GCD), and electrochemical impedance spectroscopy (EIS). The PCG ternary nanocomposite exhibits a specific capacitance of 183 F g⁻¹ at 1 A g⁻¹ in a two-electrode device, and retains its 93% of initial specific capacitance after 2000 cycles. The energy density of PCG ternary nanocomposite is 49.81 Wh Kg⁻¹ with a power density of 697.72 W Kg⁻¹. The excellent electrochemical properties of the PCG ternary nanocomposite are credited to the good contact and the synergistic effect between the PANI nanofibers, Co₃O₄ nanoparticles, and graphene nanosheets. This indicates that this synthesized ternary nanocomposite material could be used as a promising candidate for supercapacitor electrode material.

✉ Imran Murtaza
imran.murtaza@iiu.edu.pk

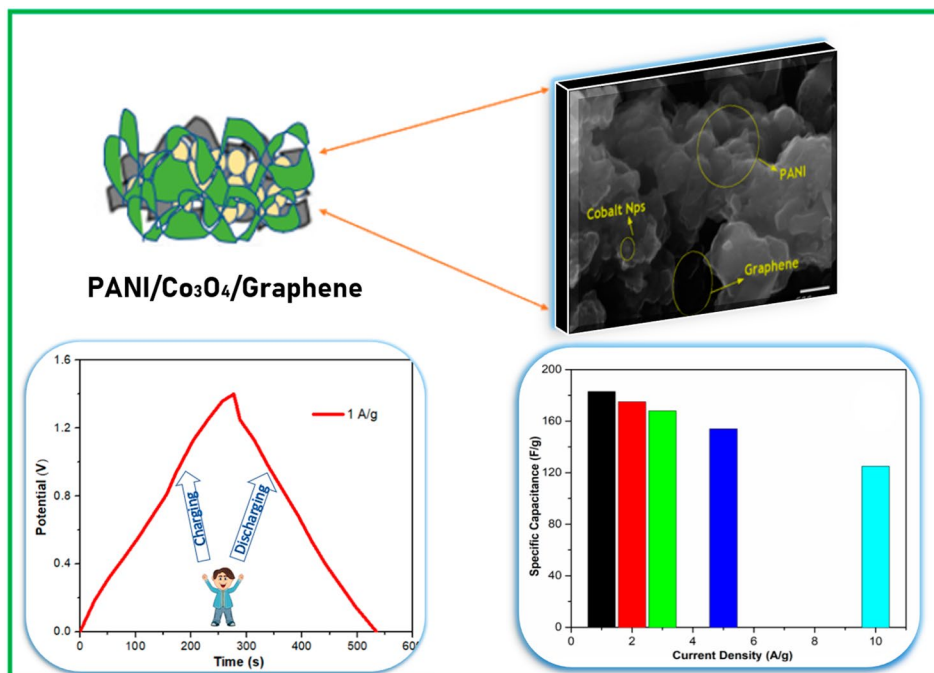
¹ Department of Physics, International Islamic University, Islamabad 44000, Pakistan

² Centre for Advanced Electronics & Photovoltaic Engineering (CAEPE), International Islamic University, Islamabad 44000, Pakistan

³ Nanosciences and Technology Department, National Center for Physics, QAU Campus, Islamabad 45320, Pakistan

⁴ Department of Chemistry, Quaid-i-Azam University, Islamabad 45320, Pakistan

Graphical Abstract



Keywords PANI · nanocomposite · graphene · supercapacitor · polymerization

Introduction

Depleted resources of fossil fuels has triggered scientists and governments to focus on alternative resources of energy. The availability of non-conventional energy resources and the immense work on them demand the development of novel materials for efficient energy storage devices. The promising alternative in this arena is electrochemical energy storage systems, which comprise fuel cells, rechargeable batteries, and supercapacitors. A supercapacitor is one of the energy storage devices that can store charges in a short time. Supercapacitors are different from batteries, which can hold huge amounts of energy, whereas supercapacitors have more power density and short durations of charge/discharge and long cycle life as compared to batteries.¹ Supercapacitors based on novel electrode materials with high-performance electrochemical features are the primary emphasis of contemporary scientists' interest.^{2,3} Supercapacitors are divided into two main types, due to their mechanism of charging and discharging and the materials used, i.e., the electrochemical double-layer capacitor (EDLC) and the pseudocapacitors.^{4,5} In EDLCs, the electrode materials are mostly carbon-based like graphene, having high power density and long cycle life, but these materials contain low specific capacitance values which confine their applications. However, pseudocapacitors use conducting polymers and transition metal oxides

(TMOs) as electrode material for enhanced capacitance as compared to the EDLCs. The hybrid material of EDLCs and pseudocapacitors containing all types of electroactive material is a better way to achieve the best electrochemical properties.⁶ Nowadays, the energy density of a supercapacitor is an important parameter, hence research is being focused on increasing it. There are two approaches, one is to enhance the specific capacitance by making a composite with materials having high specific capacitance, and the second approach is to increase the operating potential window.

Different types of electrolytes are being used, mainly aqueous electrolytes, ionic liquids, organic electrolytes, and solid-state electrolytes.^{7–10} The electrolyte is generally selected containing properties of cost-effectiveness and minimal toxicity, a high potential window, non-corrosive, high electrochemical stability, good ionic conductivity, low leakage current, and temperature stability. Encompassing all these parameters in neutral aqueous electrolytes with extended potential windows are preferred. Halder¹¹ has achieved excellent electrochemical results by an extended potential window of (–1 V to 1 V), (–0.8 V to 0.8 V), and (–1 V to 1 V) for MOs/PANI/graphene (MOs: ZrO₂, WO₃, and V₂O₅) in 1 M neutral aqueous electrolyte of Na₂SO₄ in a three-electrode system. Among conducting polymers, polyaniline (PANI) is one of the most significant materials for supercapacitor electrodes due to its excellent capacity for

energy storage, higher electrical conductivity, good environmental stability, cost-effectiveness, and easy synthesis.^{12–15} TMOs also have high pseudo-capacitance but the lack of conductivity is a major drawback that can be compensated in the hybrid with EDLCs material like graphene. Cobalt oxide (Co₃O₄) is a favorable candidate with high theoretical capacitance (3560 F/g), and its hybrid with graphene can also be compensated for the low conductivity of Co₃O₄.¹⁶ Graphene is a very attractive EDLC material due to many interesting properties, like high mechanical strength, thermal stability,¹³ and high electrical conductivity, as well as an astonishingly high theoretical specific surface area of 2630 cm² g⁻¹.^{17–19} However, graphene has a drawback of re-stacking of the sheets, which reduces the surface area and specific capacitance. This drawback can be overcome by making composites with metal oxides.²⁰ Metal oxides hinder the restacking of sheets by incorporating them between the sheets. As a result, in a ternary nanocomposite, when pseudocapacitive materials such as PANI and graphene are used with Co₃O₄, the overall specific capacitance and other electrochemical properties are enhanced. In this work, we adopt a cost-effective chemical synthesis route for the preparation of ternary PANI/Co₃O₄/graphene (PCG) nanostructure as an electrode material for supercapacitors, and report a high specific capacitance of PCG with enhanced energy density in 1 M neutral aqueous electrolyte of Na₂SO₄. This technique may be further extended at the industrial scale for the fabrication of devices.

Experimental

Materials

Aniline, cobalt chloride hexahydrate (CoCl₂·6H₂O), graphene, ammonium persulfate ((NH₄)₂S₂O₈), hydrochloric acid (HCl), cobalt chloride hexahydrate (CoCl₂·6H₂O), ammonium hydroxide (NH₄OH), sodium hydroxide (NaOH), and acetone were purchased from Sigma Aldrich. Double-distilled water was obtained from the setup installed in the laboratory.

Preparation of PANI and Co₃O₄

PANI was obtained by the chemical polymerization method. First, 50 ml of water was taken in a beaker and 7 ml of HCl was added to it and cooled to 0°C. After that, 1.45 ml of aniline was added gradually by pipette which immediately started the polymerization process. Then, 2.24 g of ammonium persulfate (APS) was dissolved in 20 ml of water in a separate beaker and gradually added to the initial solution. Then, the resultant solution was allowed to stir for 18 h at 0°C to obtain the maximum yield. After that, the

solution was dried at 60°C overnight and dried powder was obtained. The Co₃O₄ nanoparticles were synthesized by the co-precipitation method in which 4.76 g of CoCl₂·6H₂O was dissolved in 100 ml of water in a beaker under a magnetic stirrer. Then, 4 g of NaOH was dissolved in 20 ml of water in a separate beaker and gradually dropped into the CoCl₂ solution. Precipitates appeared in the final solution due to an exothermic reaction, and this solution was allowed to stir for 3 h. After that, the solution was allowed to cool at room temperature and then centrifuged many times to remove unnecessary chlorides from the precursor. The obtained solution was dried in the oven for 18 h at 80°C, and then ground to obtain powder which was subsequently sintered at 200°C.

Preparation of Binary PANI/Co₃O₄ (PC) and Co₃O₄/Graphene (CG)

The composite of PANI/Co₃O₄ (PC) was synthesized by the chemical polymerization method as mentioned above. The pre-synthesized cobalt oxide nanoparticles were ultra-sonicated for 1 h in water for good dispersion, and then this solution was incorporated into hydrochloric acid solution, followed by the same process to obtain the PC binary nanocomposite. For the Co₃O₄/graphene (CG) binary nanocomposite, 50 mg of graphene was added to 100 ml of distilled water and ultra-sonicated for 2 h. At the same time, 0.5 M of CoCl₂·6H₂O was added to 20 ml of water and stirred vigorously for 1 h. The obtained solution was mixed with the suspension of graphene and again ultra-sonicated for 1 h, and eventually put on a hot plate for stirring. Ammonium hydroxide was gradually added to the above solution by pipette until pH 9 and remained being stirred for the next 5 h. After that, the solution was centrifuged and washed several times with distilled water to obtain black precipitates. The obtained solution was dried at 70°C overnight and ground to obtain a fine powder of the Co₃O₄/graphene nanocomposite and subsequently sintered at 200°C.

Preparation of PANI/Co₃O₄/Graphene Ternary Nanocomposite (PCG)

Figure 1 shows a schematic for the synthesis of the ternary nanocomposite. For the PCG nanocomposite, the same chemical polymerization method was used as mentioned above. The ternary composite was obtained with a suitable ratio by weight of aniline and the as-synthesized Co₃O₄-graphene binary nanocomposite. Aniline and Co₃O₄-graphene were utilized in an 80:20 weight ratio. First, 4.8 ml aniline and 1.2 mg of the Co₃O₄-graphene composite were added to 100 ml of water and ultra-sonicated for 1 h, and then a pre-cooled solution of APS and HCl was injected and finally sonicated for 1 h, followed by a repetition of

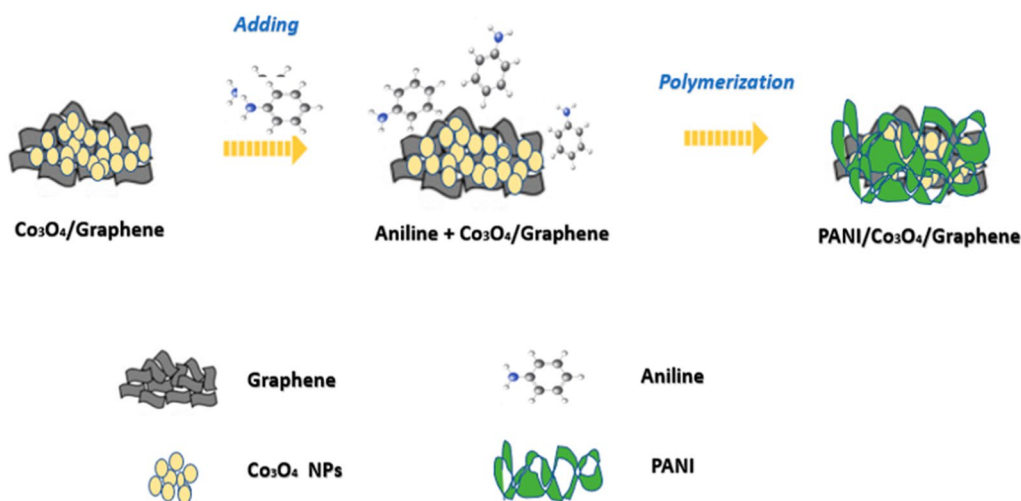


Fig. 1 Schematic of the synthesis of the ternary PCG nanocomposite.

the above polymerization method to obtain the ternary nanocomposite.

Electrochemical Measurement and Analysis

For the electrochemical measurements, a Gamry AutoLab potentiostat/galvanostat system connected to a three-electrode cell in a 1 M Na_2SO_4 solution was utilized for cyclic voltammogram (CV) and electrochemical impedance spectroscopy (EIS). Ni foam was used as a working electrode (WE) whereas platinum wire and silver chloride were used as counter and reference electrodes, respectively. To deposit the sample on the WE, first Ni foam with an area of $1 \times 1 \text{ cm}^2$ was washed with distilled water and ethanol before sonication for 10 min. Then 80 wt% of the active material (PCG), 10 wt% of activated carbon, and 10 wt% of polyvinylidene fluoride were dispersed in 1-methyl-2-pyrrolidone to obtain a homogenous slurry. The slurry was added dropwise on Ni foam (WE) with the help of a micropipette and dried overnight at 60°C . The CV measurements were taken in a potential window of -0.4 V to 1 V . The EIS, a non-destructive technique, was used to check the electrode kinetics in an open circuit potential with an ac amplitude of 5 mV from 1000 k to 0.1 Hz in a three-electrode system. Cyclic stability of the PCG composite was checked by repeating the galvanostatic charge-discharge (GCD) measurement for 2000 cycles. A two-electrode symmetric device was fabricated for the GCD measurements, and electrodes prepared for GCD are in the same manner as mentioned above for the CV measurements. The mass of each electrode is about 5 mg , including conducting agent and binder. The following equation was used to calculate the specific capacitance (C_s) from the GCD graphs:^{21,22}

$$C_s = \frac{I \times \Delta t}{m \times \Delta V} \quad (1)$$

where C_s is the specific capacitance (F g^{-1}), I is the charge/discharge current (A), Δt is the discharge time (s), m is the mass of active materials (g) for both electrodes, and ΔV represents the voltage change during the discharge process (V).

Results and Discussion

XRD Analysis

The XRD pattern of the s-synthesized PCG ternary nanocomposite is illustrated in Fig. 2. The diffraction peaks of the CG nanocomposites are shown in Fig. 2a, with the inset exhibiting the XRD pattern of the Co_3O_4 nanoparticles. Graphene exhibits diffraction peaks at 26.5° and 54.6° , corresponding to the (002) and (004) planes. Further peaks at 19.1° , 31.4° , 36.8° , 38.7° , 44.9° , 55.7° , 59.5° , 65.3° , and 77.3° corresponding to the (111), (220), (311), (222), (400), (422), (511), (440), and (533) planes, respectively, are attributed to the cubic assembly of Co_3O_4 nanoparticles matched with JCPDS # 42-1467. The Scherrer equation has been used to determine the crystallite size of the Co_3O_4 nanoparticles corresponding to the (311) peak, which was found to be 52.3 nm .²³ The diffraction peaks of the PC nanocomposites are shown in Fig. 2b, with the inset showing the XRD pattern of the PANI. PANI, which is semi-crystalline, reveals two prominent peaks at 25.3° and 20.1° correlating to the lattice planes 322, and 113, demonstrating that most PANI strands are arranged in such two lattice planes, matched with JCPDS # 72-0634.^{24,25} Further peaks of Co_3O_4 are clearly seen in the PC nanocomposite.

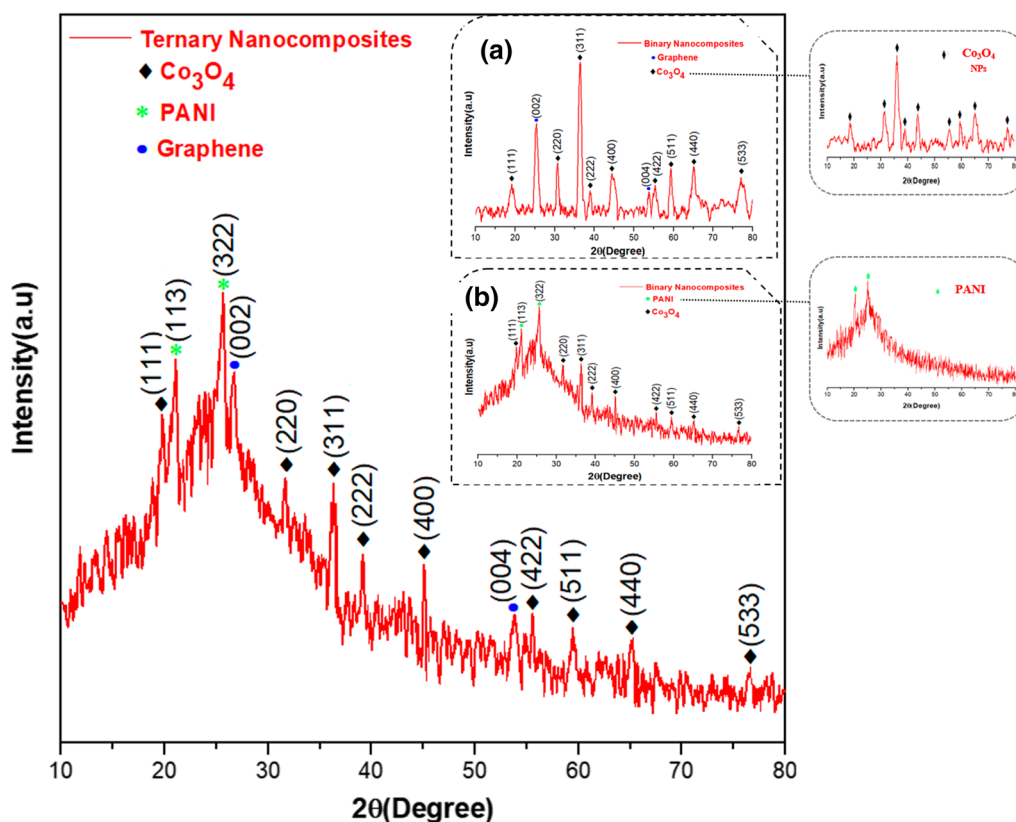


Fig. 2 XRD pattern of PANI/Co₃O₄/graphene (PCG) ternary nanocomposite. (a) Co₃O₄/graphene (CG) nanocomposites; *inset* XRD pattern of Co₃O₄ nanoparticles. (b) PANI/Co₃O₄ (PC) nanocomposites; *inset* XRD pattern of polyaniline (PANI).

Finally, prominent peaks can be clearly seen in the XRD pattern of the PCG ternary nanocomposite, indicating the successful incorporation of Co₃O₄ nanoparticles into the ternary PCG composite. These results indicate that the PCG ternary nanocomposite is primarily crystalline in nature.

FTIR Analysis

FTIR spectra of PANI, Co₃O₄, PC, CG, and PCG ternary nanocomposites are displayed in Fig. 3, in the frequency range of 500 cm⁻¹–3500 cm⁻¹. The main absorption peaks at 1556 and 1473 cm⁻¹ are due to C=C stretching modes in the quinoid and benzenoid structure for the emeraldine salt of polyaniline. The peaks at 1291 cm⁻¹, 980 cm⁻¹, and 670 cm⁻¹ are responsible for the C–N stretching mode, C=N stretching mode, and C–C stretching mode in the benzenoid structure, respectively.^{26,27} The peaks at 674 cm⁻¹ and 569 cm⁻¹, verify the formation of Co₃O₄ nanoparticles, which might be responsible for the M–O stretching modes, where M has a Co³⁺ octahedral and a Co²⁺ tetrahedral arrangement.²⁸ The FTIR spectra of the PC nanocomposite are nearly equivalent to PANI with a slight shift in Co₃O₄ peaks due to the semi-crystalline nature of PANI. The peak at 1614

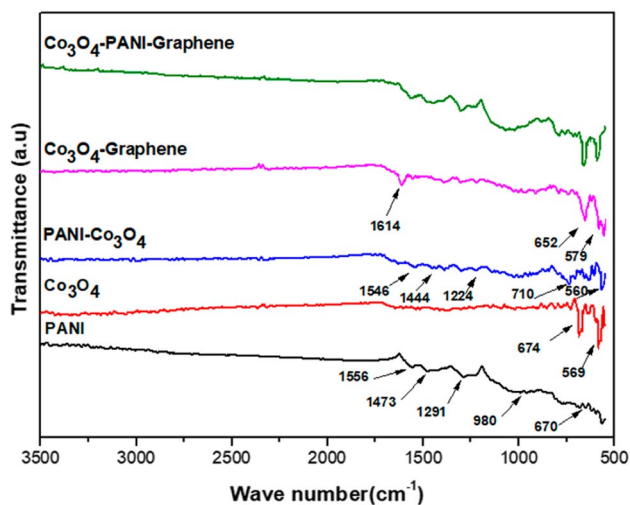


Fig. 3 FTIR spectra of PANI, Co₃O₄, PANI/Co₃O₄, Co₃O₄/graphene, and PANI/Co₃O₄/graphene ternary nanocomposite.

cm⁻¹ in CG is attributed to graphitic C=C vibration modes.²⁹ Stretching bands in the FTIR results further confirm the successful synthesis of the PCG ternary nanocomposite.

Morphological Analysis of PANI/Co₃O₄/Graphene (PCG)

The SEM results portray the morphologies of Co₃O₄ nanoparticles, polyaniline, binary PC, and CG nanocomposites,

and PCG ternary nanocomposites in Fig. 4a–f and g–k, revealing the EDX spectroscopy results of all the prepared materials. Figure 4a represents porous cobalt oxide nanoparticles and Fig. 4g shows the mapping of elemental cobalt. These Co₃O₄ nanoparticles are distributed in the PANI

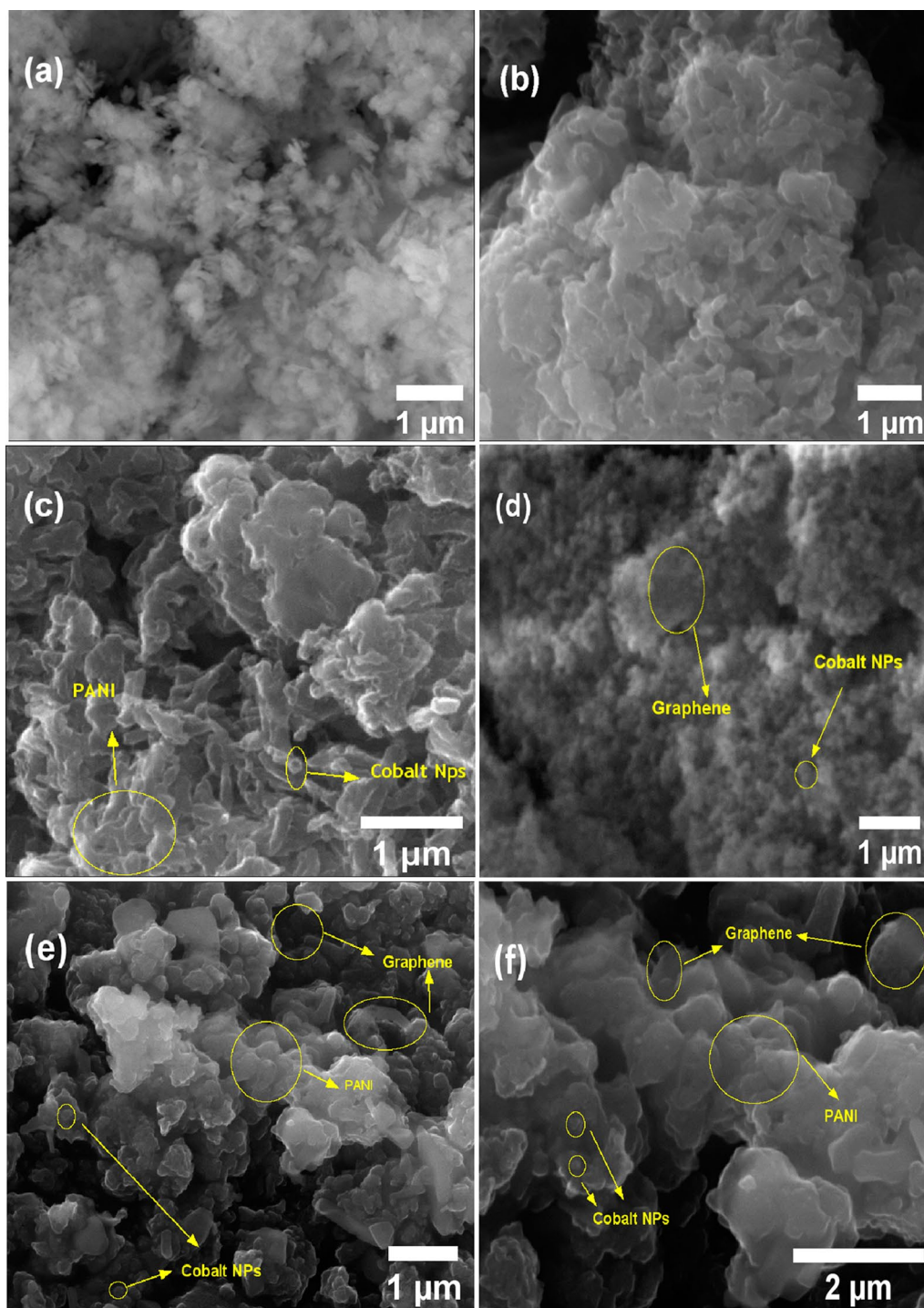


Fig. 4 SEM images of (a) Co₃O₄ NPs, (b) PANI, (c) PANI/Co₃O₄ nanocomposite, (d) Co₃O₄/graphene nanocomposite, and (e, f) PANI/Co₃O₄/graphene nanocomposites at different resolutions. Elemental

mapping of (g) Co₃O₄ NPs, (h) PANI, (i) PANI/Co₃O₄ nanocomposite, (j) Co₃O₄/graphene nanocomposite, and (k) PANI/Co₃O₄/graphene nanocomposite.

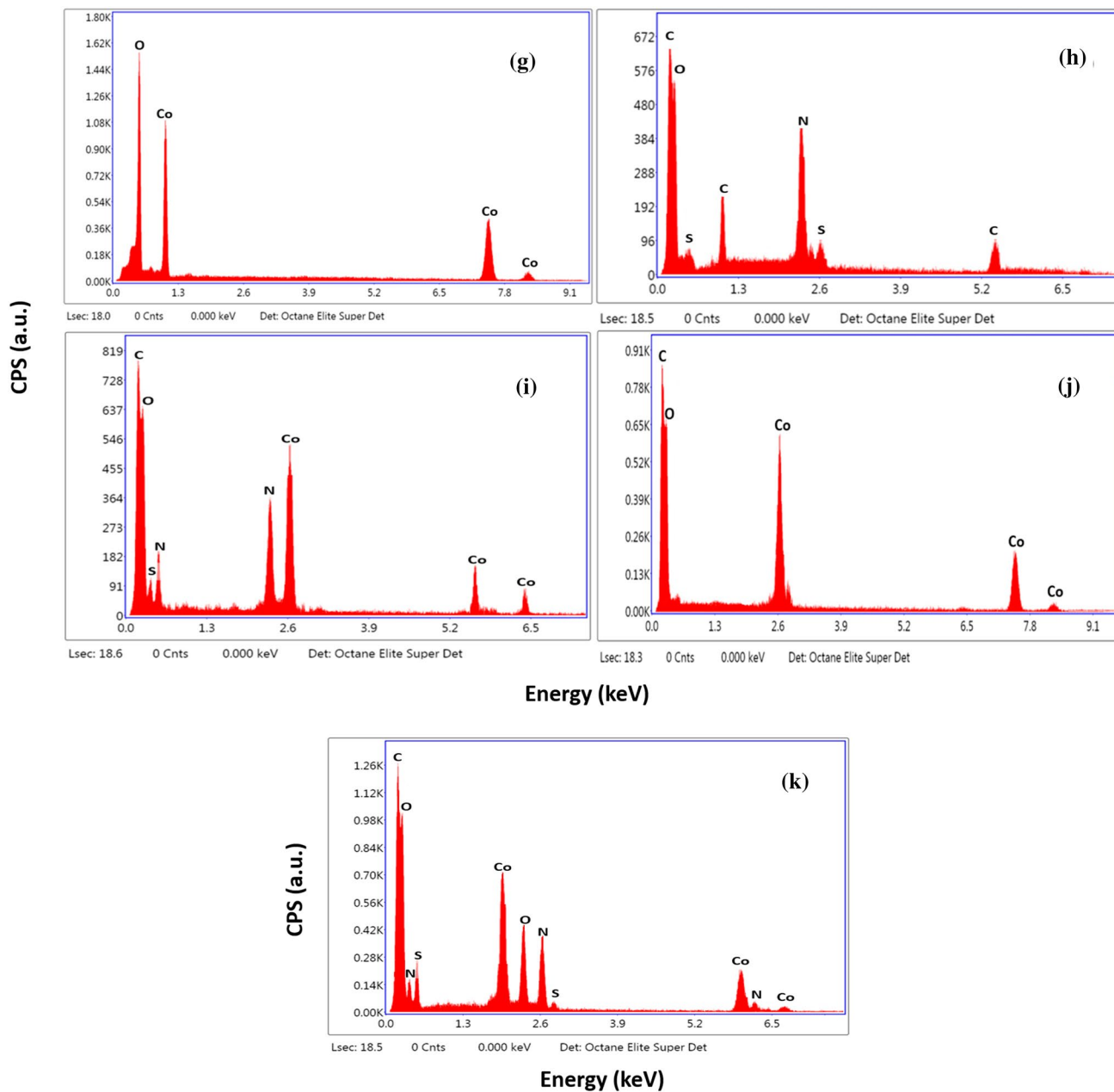


Fig. 4 (continued)

nanofibrous structure in the binary PC nanocomposite, as shown in Fig. 4c, which is also indicated by its elemental mapping in Fig. 4i. The existence of sulfur is analyzed in the EDX of PANI, as shown in Fig. 4h. The elemental distribution of S, C, O, and N in the PANI has been revealed. The element S is attributed to ammonium persulfate that is utilized in the polymerization process, whereas the elements C, O, and N are credited to the PANI. The SEM image of CG is shown in Fig. 4d, indicating the existence of tiny nanoparticles of Co₃O₄ evenly disseminated on the graphene nanosheets, illustrating strong interaction between

cobalt oxide nanoparticles and graphene nanosheets. Figure 4j demonstrates the presence of graphene and cobalt oxide from its elemental mapping data. These cobalt oxide nanoparticles may also act as a spacer and hinder the stacking of graphene sheets. The binary CG nanocomposite used in the ternary PCG may also act as a nanofiller for PANI in the composite, which may help in the hindrance of volume changing during continuous cycles of charging and discharging. The synthesized PCG ternary nanocomposites show a synergistic effect, and can be used for charge storage applications. Figure 4e, f depicts the presence of a PANI-dominated

PCG network and cobalt oxide nanoparticles in graphene nanosheets at different resolutions. The distributions of C, O, N, S, and Co are shown in Fig. 4k. The distribution of N in the PCG structure suggests the presence of a PANI network, and supports the SEM results. As a result, element mapping reveals the distinct ternary nanostructure of PCG. Hence, the EDX results demonstrate the existence of constituent elements in the synthesized material that validate the SEM results.

Electrochemical Investigations

Figure 5a depicts the electrochemical properties of Co_3O_4 , CG, and PCG ternary nanocomposites examined by CV at a scan rate of 20 mV s^{-1} in $1 \text{ M Na}_2\text{SO}_4$ in a three-electrode system. CV shows a small deviation from a rectangular shape in Co_3O_4 , PC, and PCG ternary nanocomposites, leading to the conclusion that pseudocapacitive behavior based on a faradaic mechanism exists.^{30,31} Figure 5b shows the CV curves of PCG nanocomposites at various scan rates from 10 to 100 mV s^{-1} . Good reversibility and electrochemical behavior with an increased scan rate of the PCG nanocomposite network suggest the strong synergistic effect between PANI, cobalt oxide, and graphene nanostructures. Elevating the scan rate of the PCG nanocomposite leads to a decrease in the specific capacitance, because, at a small scan rate, ions were well propagated into inner active regions of the PCG ternary nanocomposite, resulting in better charge transfer that effectively triggers the redox process. However, at a large scan rate, ions cannot effectively permeate into the inner active regions of the PCG ternary nanocomposite, and hence redox processes are limited.^{32,33}

The electrochemical impedance is a useful technique for the frequency response analysis of the electrochemical

characteristics of electrode material. The Nyquist plot is shown in Fig. 6 for Co_3O_4 , CG, and PCG which have been tested in $1 \text{ M Na}_2\text{SO}_4$ in the frequency range between 1000 kHz and 0.1 Hz . The intercept on the real impedance axis gives the resistance R_s , which is collectively taken as the resistance of the electrolyte in solution and the internal electrode resistance.^{21,34} The R_s value for PCG is 4.58Ω and for Co_3O_4 and CG is 3.48Ω and 2.82Ω , respectively. Nyquist curves in the high-frequency region display a semicircle, and show a relatively linear response at mid- and low frequencies. The radius of the semicircle describes the charge-transfer resistance (R_{ct}) which is associated with the processes at the electrode–electrolyte interface, and the sloped line displayed at mid-frequencies is due to Warburg

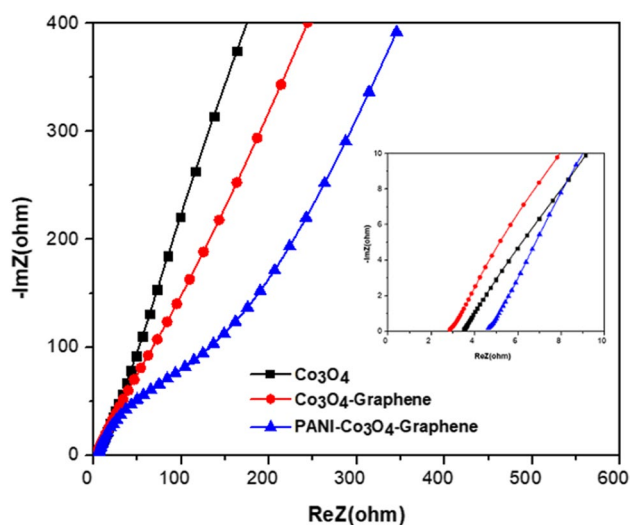


Fig. 6 Nyquist plot for Co_3O_4 , $\text{Co}_3\text{O}_4/\text{graphene}$, and $\text{PANI}/\text{Co}_3\text{O}_4/\text{graphene}$ in $1 \text{ M Na}_2\text{SO}_4$ solution in a three-electrode system.

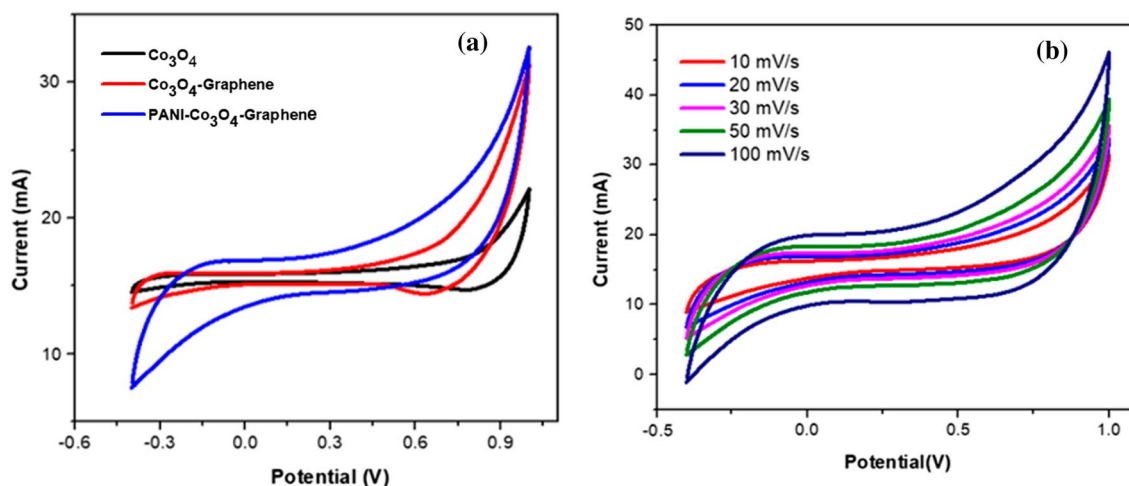


Fig. 5 (a) Cyclic-voltammograms of Co_3O_4 , $\text{Co}_3\text{O}_4/\text{graphene}$, and $\text{PANI}/\text{Co}_3\text{O}_4/\text{graphene}$ nanocomposites at 20 mV s^{-1} , and (b) PCG ternary nanocomposites with varied scan rates ($10, 20, 30, 50,$ and 100 mV s^{-1}).

diffusion, indicating the diffusion of ions into the electrode.³⁵ Therefore, the improved electronic activity of the PCG ternary composite with good electrical conductivity of the entire electrode promotes the charge–discharge activity.

To investigate the energy density and power density of the synthesized nanocomposite, GCD was carried out for the PCG two-electrode symmetrical device at different current densities. The GCD curves of the PCG nanocomposite are shown in Fig. 7a at current densities of 1 A g⁻¹, 2 A g⁻¹, 3 A g⁻¹, 5 A g⁻¹, and 10 A g⁻¹ respectively. The specific capacitance has been calculated using Eq. 1 and the values are 183, 175 F g⁻¹, 168 F g⁻¹, 154 F g⁻¹, and 125 F g⁻¹, respectively. Figure 7b shows GCD curves of PCG, CG, and PC at 1 A g⁻¹. With increasing current density, the specific capacitance decreases, as shown in Fig. 7c, because at high current rates the electrolyte ions do not find enough time to interact with the inner active sites rather the ions only interacting with the surface of the nanocomposite.^{36,37} In Fig. 7d, the PCG capacitance retention is plotted as a function of cycle number, displaying

excellent capacitance retention over 2000 cycles, with the PCG nanocomposite sustaining a capacitance of up to 93 % at 2 A g⁻¹.

The parameters such as energy density and power density have been calculated using Eqs. 2 and 3 for a two-electrode system:

Table 1 Electrochemical parameters of two-electrode symmetric devices

| Current density (A g ⁻¹) | Specific capacitance (F g ⁻¹) | Energy density (Wh Kg ⁻¹) | Power density (W Kg ⁻¹) |
|--------------------------------------|---|---------------------------------------|-------------------------------------|
| 1 | 183 | 49.81 | 697.72 |
| 2 | 175 | 47.63 | 1394.04 |
| 3 | 168 | 45.73 | 2138.02 |
| 5 | 154 | 42.01 | 3780.90 |
| 10 | 125 | 34.02 | 12247.21 |

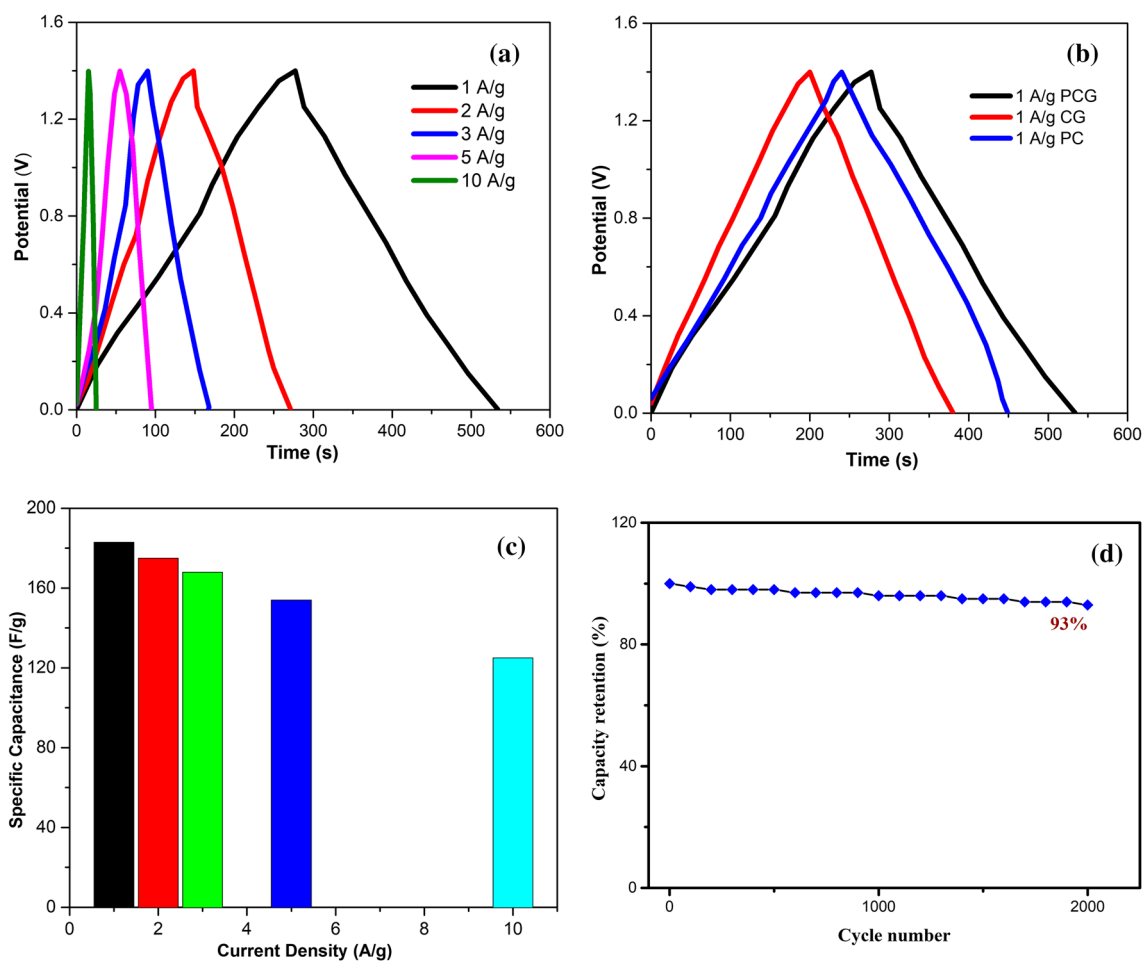


Fig. 7 (a) GCD curves of the PCG composite at different current densities, (b) GCD curves of PCG, CG, and PC at 1 A g⁻¹. (c) Specific capacitance values as a function of current density, and (d) PCG capacitance retention over 2000 cycles.

Table II Comparison of energy and power densities of different materials in a two-electrode system

| Materials | Energy density (Wh Kg ⁻¹) | Power density (W Kg ⁻¹) | Electrolyte | References |
|---|---------------------------------------|-------------------------------------|-------------------------------------|--------------|
| rGO/V ₂ O ₅ | 31.3 | 249.7 | 1 M Na ₂ SO ₄ | 38 |
| Co ₃ O ₄ -rGO | 20 | 1200 | 1 M KOH | 39 |
| Co ₃ O ₄ /MnO ₂ | 24.37 | 450 | 1 M Na ₂ SO ₄ | 40 |
| CoTiO ₃ @Co ₃ O ₄ /N-CNO | 34.7 | 2190 | 2 M KOH | 41 |
| GO/Co ₃ O ₄ /NiO | 17.77 | 394.94 | 1 M Na ₂ SO ₄ | 42 |
| Graphene/polyaniline@carbon | 11.38 | 199.8 | 1 M H ₂ SO ₄ | 43 |
| PANI/Co ₃ O ₄ /graphene (PCG) | 49.81 | 697.72 | 1 M Na ₂ SO ₄ | Present work |

$$E = \frac{1}{2} \times \frac{CV^2}{3.6} \quad (2)$$

$$P = \frac{E}{t} \times 3600 \quad (3)$$

The symmetrical device shows energy densities of 49.81, 47.63, 45.73, 42.01, and 34.02 Wh Kg⁻¹ at power densities of 697.72, 1394.04, 2138.02, 3780.90, and 12,247.21 W Kg⁻¹ respectively. Thus, the energy density of the synthesized PCG nanocomposite is 49.81 Wh Kg⁻¹, which is superior to the energy density of the PC and CG composites, which are 39.95 and 35.19 Wh Kg⁻¹, respectively, as shown in Fig. 7b at 1 A g⁻¹. Table I shows the electrochemical parameters of two-electrode symmetric devices.

In Table II, a comparison of the energy and power densities of different materials in a two-electrode system have been illustrated, primarily in aqueous electrolytes. The results obtained in this work for the PCG composite demonstrate improved electrochemical performance, as shown in Table II. The synergistic effect of PANI, graphene, and Co₃O₄ may be responsible for the enhancement of the electrochemical performance in the PCG nanocomposite. PANI is a conducting polymer that has a diverse redox mechanism, high conductivity, and high energy density, and shows high pseudo-capacitance. A PANI coating on Co₃O₄ can extend its cyclic life by providing more electron carriers or channels, as well as assist in polymer degradation problems. Furthermore, graphene is used in composites due to its excellent conductivity, mechanical stability, high surface area, high power density, and long cycle life, compared with any other carbonaceous material. However, the restacking of graphene nanosheets and its low specific capacitance value limit its applications. These limitations of graphene can be overcome by making its composite with PANI and Co₃O₄ to enhance the specific capacitance. PANI and Co₃O₄ provide hindrance in the restacking of graphene nanosheets by acting as a spacer as well as enhancing the specific capacitance, but these materials lack good conductivity and cyclic stability. Therefore, a ternary PCG composite comprising graphene,

PANI, and Co₃O₄ is responsible for enhanced electrochemical performance in aqueous 1 M Na₂SO₄ for supercapacitor applications.

Conclusions

A facile and cost-effective route was used to synthesize a PANI/Co₃O₄/graphene (PCG) ternary nanocomposite for supercapacitor applications, with a wider potential window of 1.4 V in 1 M Na₂SO₄ solution. In the complex PCG structure, Co₃O₄ nanoparticles hinder restacking of graphene sheets, which consequently helps in the favorable mobility of the ions. Also, the morphology indicates that a complex network is suitable for more ion diffusion from the electrolyte to the electrode material. Therefore, the PCG material shows a good specific capacitance of 183 F g⁻¹ at 1 A g⁻¹, and reveals a high energy density of 49.81 Wh Kg⁻¹ at a power density of 697.72 W Kg⁻¹ in an aqueous 1 M Na₂SO₄ electrolyte in a two-electrode system. Furthermore, the PCG nanocomposite shows good cyclic stability and retains 93% of its initial capacitance after 2000 charge/discharge cycles at 2 A g⁻¹. Thus, the facile and cost-effective route employed to synthesize the PCG ternary nanocomposite, showing good capacitance and enhanced energy density in aqueous 1 M Na₂SO₄ electrolyte, could pave the way to upscale the proposed technology.

Acknowledgments We would like to acknowledge funding from Higher Education Commission Pakistan, Grant No. 20-ICRG-165/RGM/HEC/2020, and Pakistan Science Foundation, Grant No. PSF/NSFC-II/ENG/C-IIUI-06. We are also grateful to Prof. Dr. Syed Rizwan Hussain (NUST) and Prof. Dr. Asim Rashid (PIEAS) for assistance with Cyclic-Voltammetry and SEM respectively.

Conflict of interest The authors declare no conflict of interest.

References

1. L.Q. Fan, G.J. Liu, J.H. Wu, L. Liu, J.M. Lin, and Y.L. Wei, Asymmetric supercapacitor based on graphene oxide/polypyrrole

- composite and activated carbon electrodes. *Electrochim. Acta.* 137, 26 (2014).
2. L. Zhang, K.N. Hui, K.S. Hui, X. Chen, R. Chen, and H. Lee, Role of graphene on hierarchical flower-like NiAl layered double hydroxide-nickel foam-graphene as binder-free electrode for high-rate hybrid supercapacitor. *Int. J. Hydrog. Energy* 41, 9443 (2016).
 3. S. Vijayakumar, S. Nagamuthu, S.H. Lee, and K.S. Ryu, Porous thin layered nanosheets assembled ZnCo₂O₄ grown on Ni-foam as an efficient electrode material for hybrid supercapacitor applications. *Int. J. Hydrog. Energy* 42, 3122 (2017).
 4. R. Singh, and C.C. Tripathi, Electrochemical exfoliation of graphite into graphene for flexible supercapacitor application. *Mater. Today: Proc.* 5, 1125 (2018).
 5. Y. Liu, I. Murtaza, A. Shuja, and H. Meng, Interfacial modification for heightening the interaction between PEDOT and substrate towards enhanced flexible solid supercapacitor performance. *Chem. Eng. J.* 379, 122326 (2020).
 6. K. Makgopa, P.M. Ejikeme, C.J. Jafta, K. Raju, M. Zeiger, V. Presser, and K.I. Ozoemena, A high-rate aqueous symmetric pseudocapacitor based on highly graphitized onion-like carbon/birnessite-type manganese oxide nanohybrids. *J. Mater. Chem. A.* 3, 3480 (2015).
 7. X. Zhang, X. Wang, L. Jiang, H. Wu, C. Wu, and J. Su, Effect of aqueous electrolytes on the electrochemical behaviors of supercapacitors based on hierarchically porous carbons. *J. Power Sources* 216, 290 (2012).
 8. F. Wang, X. Wu, X. Yuan, Z. Liu, Y. Zhang, L. Fu, Y. Zhu, Q. Zhou, Y. Wu, and W. Huang, Latest advances in supercapacitors: from new electrode materials to novel device designs. *Chem. Soc. Rev.* 46, 6816 (2017).
 9. X. Cheng, J. Pan, Y. Zhao, M. Liao, and H. Peng, Gel polymer electrolytes for electrochemical energy storage. *Adv. Energy Mater.* 8, 1702184 (2018).
 10. C. Zhong, Y. Deng, W. Hu, J. Qiao, L. Zhang, and J. Zhang, A review of electrolyte materials and compositions for electrochemical supercapacitors. *Chem. Soc. Rev.* 44, 7484 (2015).
 11. P. Haldar, Achieving wide potential window and high capacitance for supercapacitors using different metal oxides (viz.:ZrO₂, WO₃ and V₂O₅) and their PANI/graphene composites with Na₂SO₄ electrolyte. *Electrochim. Acta.* 381, 1382 (2021).
 12. M. Nallappan, and M. Gopalan, Fabrication of CeO₂/PANI composites for high energy density supercapacitors. *Mater. Res. Bull.* 106, 357 (2018).
 13. S. Islam, G.B.V.S. Lakshmi, A.M. Siddiqui, M. Husain, and M. Zulfeqar, Synthesis, electrical conductivity, and dielectric behavior of polyaniline/V₂O₅ composites. *Int. J. Polym. Sci.* 2013, 1–7 (2013).
 14. R. Li, H. Xu, R. Fu, W. Tan, Y. Qin, Y. Tao, and Y. Kong, Preparation of 3D reduced graphene oxide/carbon nanospheres/polyaniline ternary nanocomposites as supercapacitor electrode. *React. Funct. Polym.* 125, 101 (2018).
 15. P. Asen, and S. Shahrokhian, Ternary nanostructures of Cr₂O₃/graphene oxide/conducting polymers for supercapacitor application. *J. Electroanal. Chem.* 823, 505 (2018).
 16. R. Kumar, H.J. Kim, S. Park, A. Srivastava, and I.K. Oh, Graphene-wrapped and cobalt oxide-intercalated hybrid for extremely durable super-capacitor with ultrahigh energy and power densities. *Carbon* 79, 192 (2014).
 17. C. Lee, X. Wei, J.W. Kysar, and J. Hone, Measurement of the elastic properties and intrinsic strength of monolayer graphene. *Science* 321, 385 (2008).
 18. D.S. Ghosh, I. Calizo, D. Teweldebrhan, E.P. Pokatilov, D.L. Nika, A.A. Balandin, W. Bao, F. Miao, and C.N. Lau, Extremely high thermal conductivity of graphene: prospects for thermal management applications in nanoelectronic circuits. *Appl. Phys. Lett.* 92, 151911 (2008).
 19. M. Orlita, C. Faugeras, P. Plochocka, P. Neugebauer, G. Martinez, D.K. Maude, A.L. Barra, M. Sprinkle, C. Berger, W.A. de Heer, and M. Potemski, Approaching the Dirac point in high-mobility multilayer epitaxial graphene. *Phys. Rev. Lett.* 101, 267601 (2008).
 20. Z.S. Wu, G. Zhou, L.C. Yin, W. Ren, F. Li, and H.M. Cheng, Graphene/metal oxide composite electrode materials for energy storage. *Nano Energy* 1, 107 (2012).
 21. A. Jeyaranjan, T.S. Sakhthivel, C.J. Neal, and S. Seal, Scalable ternary hierarchical microspheres composed of PANI/rGO/CeO₂ for high performance supercapacitor applications. *Carbon* 151, 192 (2019).
 22. C. Huang, C. Hao, W. Zheng, S. Zhou, L. Yang, X. Wang, C. Jiang, and L. Zhu, Synthesis of polyaniline/nickel oxide/sulfonated graphene ternary composite for all-solid-state asymmetric supercapacitor. *Appl. Surf. Sci.* 505, 144589 (2020).
 23. X.C. Dong, H. Xu, X.W. Wang, Y.X. Huang, M.B. Chan-Park, H. Zhang, L.H. Wang, W. Huang, and P. Chen, 3D graphene-cobalt oxide electrode for high-performance supercapacitor and enzymeless glucose detection. *ACS Nano* 6, 3206 (2012).
 24. S. Padmapriya, S. Harinipriya, K. Jaidev, V. Sudha, D. Kumar, and S. Pal, Storage and evolution of hydrogen in acidic medium by polyaniline. *Int. J. Energy Res.* 42, 1196 (2018).
 25. D.F. Acevedo, C.R. Rivarola, M.C. Miras, and C.A. Barbero, Effect of chemical functionalization on the electrochemical properties of conducting polymers. Modification of polyaniline by diazonium ion coupling and subsequent reductive degradation. *Electrochim. Acta.* 56, 3468 (2011).
 26. D. Prabakaran, K. Sadaiyandi, M. Mahendran, and S. Sagadevan, Precipitation method and characterization of cobalt oxide nanoparticles. *Appl. Phys. A* 123, 1 (2017).
 27. X. Zhou, P.H. Shi, Y.F. Qin, J.C. Fan, Y.L. Min, and W.F. Yao, Synthesis of Co₃O₄/graphene composite catalysts through CTAB-assisted method for Orange II degradation by activation of peroxymonosulfate. *J. Mater. Sci. Mater. Electron.* 27, 1020 (2016).
 28. B. Mu, W. Zhang, S. Shao, and A. Wang, Glycol assisted synthesis of graphene-MnO₂-polyaniline ternary composites for high performance supercapacitor electrodes. *Phys. Chem. Chem. Phys.* 16, 7872 (2014).
 29. B.S. Singu, and K.R. Yoon, Synthesis and characterization of MnO₂-decorated graphene for supercapacitors. *Electrochim. Acta.* 231, 749 (2017).
 30. Q. Zhou, Y. Li, L. Huang, C. Li, and G. Shi, Three-dimensional porous graphene/polyaniline composites for high-rate electrochemical capacitors. *J. Mater. Chem. A.* 2, 17489 (2014).
 31. M. Shah, I. Murtaza, R. Abid, A. Shuja, H. Meng, and N. Ahmed, Fluorene substituted thieno [3, 2-b] thiophene—a new electrochromic conjugated polymer. *J. Polym. Res.* 28, 1 (2021).
 32. F. Gopal, and M. Faraji, Electrodeposited polyaniline on Pd-loaded TiO₂ nanotubes as active material for electrochemical supercapacitor. *J. Electroanal. Chem.* 691, 51 (2013).
 33. F. Liu, S. Luo, D. Liu, W. Chen, Y. Huang, L. Dong, and L. Wang, Facile processing of free-standing polyaniline/SWCNT film as an integrated electrode for flexible supercapacitor application. *ACS Appl. Mater. Interfaces.* 9, 33791 (2017).
 34. R.B. Rakhi, W. Chen, D. Cha, and H.N. Alshareef, Substrate dependent self-organization of mesoporous cobalt oxide nanowires with remarkable pseudocapacitance. *Nano Lett.* 12, 2559 (2012).
 35. K. Wang, J. Huang, and Z. Wei, Conducting polyaniline nanowire arrays for high performance supercapacitors. *J. Phys. Chem. C.* 114, 8062 (2010).

36. J. Li, Y. Ren, Z. Ren, S. Wang, Y. Qiu, and J. Yu, Aligned polyaniline nanowires grown on the internal surface of macroporous carbon for supercapacitors. *J. Mater. Chem. A*, 3, 23307 (2015).
37. H. Lin, Q. Huang, J. Wang, J. Jiang, F. Liu, Y. Chen, C. Wang, D. Lu, and S. Han, Self-assembled graphene/polyaniline/Co₃O₄ ternary hybrid aerogels for supercapacitors. *Electrochim. Acta*, 191, 444 (2016).
38. L. Yao, C. Zhang, N. Hu, L. Zhang, Z. Zhou, and Y. Zhang, Three-dimensional skeleton network so reduced graphene oxide nanosheets/vanadium pentoxide nanobelts hybrid for high performance supercapacitors. *Electrochim. Acta*, 295, 14 (2019).
39. S. Raj, S.K. Srivastava, P. Kar, and P. Roy, In situ growth of Co₃O₄ nanoflakes on reduced graphene oxide-wrapped Ni-foam as high performance asymmetric supercapacitor. *Electrochim. Acta*, 302, 327 (2019).
40. V.S. Prabhin, K. Jeyasubramanian, V.S. Benitha, P. Veluswamy, and B.J. Cho, Fabrication and evaluation of hybrid supercapacitor consisting of nano cobalt oxide and manganese oxide deposited electrochemically on nanoporous Au-Electrode. *Electrochim. Acta*, 330, 135199 (2020).
41. M.R. Pallavolu, N. Gaddam, A.N. Banerjee, R.R. Nallapureddy, Y.A. Kumar, and S.W. Joo, Facile construction and controllable design of CoTiO₃@Co₃O₄/N-CNO hybrid heterojunction nanocomposite electrode for high-performance supercapacitors. *Electrochim. Acta*, 407, 139868 (2022).
42. R.M. Obodo, S.M. Mbam, H.E. Nsude, M. Ramzan, S.C. Ezike, I. Ahmad, M. Maaza, and F.I. Ezema, Graphene oxide enhanced Co₃O₄/NiO composite electrodes for supercapacitive devices applications. *Appl. Surf. Sci. Adv.*, 9, 100254 (2022).
43. L. Wen, K. Li, J. Liu, Y. Huang, F. Bu, B. Zhao, and Y. Xu, Graphene/polyaniline@carbon cloth composite as a high-performance flexible supercapacitor electrode prepared by a one-step electrochemical co-deposition method. *RSC Adv.*, 7, 7688 (2017).

Publisher's Note Springer Nature remains neutral with regard to jurisdictional claims in published maps and institutional affiliations.